JACS
JOURNAL OF THE AMERICAN CHEMICAL SOCIETY
Article
pubs.acs.org/JACS

# Electron-Donating Behavior of Few-Layer Graphene in Covalent Ensembles with Electron-Accepting Phthalocyanines

Maria-Eleni Ragoussi,[†] Georgios Katsukis,[‡] Alexandra Roth,[‡] Jenny Malig,[‡] Gema de la Torre,*[,†] Dirk M. Guldi,*[,‡] and Tomás Torres*[,†,§]

[†]Departamento de Química Orgánica, Universidad Autónoma de Madrid, Cantoblanco, Madrid 28049, Spain
[‡]Department of Chemistry and Pharmacy and Interdisciplinary Center for Molecular Materials (ICMM), Friedrich-Alexander-Universität Erlangen-Nürnberg, Erlangen 91058, Germany
[§]IMDEA-Nanociencia, c/Faraday 9, Campus de Cantoblanco, Madrid 28049, Spain

Supporting Information

**ABSTRACT:** We describe herein the first example of highly exfoliated graphene covalently linked to electron accepting phthalocyanines. The functionalization of the nanocarbon surface with alkylsulfonyl phthalocyanines was attained by means of a "click" chemistry protocol. The new ensemble was fully characterized (thermogravimetric analysis, atomic force microscopy, transmission electron microscopy and Raman, as well as ground-state absorption) and was studied in terms of electron donor–acceptor interactions in the ground and in the excited state. In particular, a series of steady-state and time-resolved spectroscopy experiments demonstrated photoinduced electron transfer from the graphene to the electron-accepting phthalocyanines. This is the first example of an electron donor–acceptor nanoconjugate, that is, few-layer graphene/phthalocyanine, pinpointing the uncommon electron donating character of graphene.

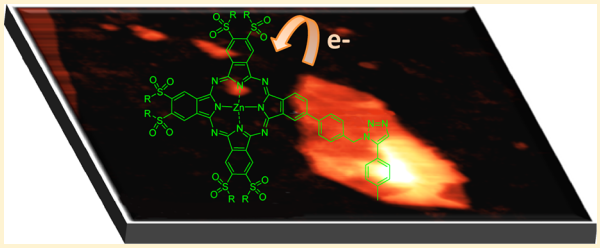


## INTRODUCTION

Graphene, a single-atom thick nanomaterial with unprecedented properties, has generated enormous interest during recent years due to its tremendous potential in the area of nanoelectronics.[1] As such, graphene is by far considered as the most promising nanostructured carbon allotrope. However, practical use of graphene is limited by its high-quality production on a large scale. Among all the methods described for the production of graphene, wet chemical exfoliation of bulk graphite is the best approach for mass production of practical single to few-layer graphene.

A sheer endless number of studies have focused on the covalent[2] and noncovalent[3] functionalization of exfoliated graphite. The thrust is not only to render it processable and dispersible in common solvents, but also to afford hybrid architectures for optoelectronic applications. In particular, linking photoactive chromophores, such as porphyrins or phthalocyanines (Pcs),[4] to single and few-layer graphene adds light harvesting, charge transfer and charge transport capabilities and, therefore, opens the potential for solar energy conversion schemes. To this date, a fairly large number of graphene–porphyrin[5] but only a few graphene–Pc hybrid architectures[6] have been reported, showing charge transfer capabilities after photoexcitation of the chromophore.

Single and few-layer graphene is usually employed as an electron acceptor when combined with a wide facet of electron donors.[7] While in the case of single-walled carbon nanotubes numerous reports have assisted in demonstrating their electron donor character *via* steady-state and time-resolved spectroscopy,[8] examples of graphene/electron acceptor hybrid architectures are less common.[9] Moreover, the electronic communication between graphene and electron acceptors was only recently demonstrated in terms of ground and excited state features.[10]

Pcs usually feature electron-donating properties after photoexcitation in covalent conjugates and/or noncovalent hybrids with carbon nanostructures such as fullerenes and carbon nanotubes.[11] Concerning graphene, noncovalent adsorption and immobilization of metalated Pcs onto epitaxially grown graphene results in weak interactions in terms of n-doping of graphene.[12] In stark contrast, we have recently reported on a covalent graphene–Pc nanoconjugate, in which the implementation of a molecular spacer decouples Pc from few-layer graphene, and gives rise to through-space, ultrafast charge separation evolving from the photoexcited Pc to graphene.[6a] Nevertheless, tailor-made electron accepting Pcs are also attainable by placing appropriate substituents at the periphery. In this regard, alkylsulfonyl groups are ideal electron-withdrawing substituents for the preparation of electron accepting Pcs[13] since they decrease the energy of the highest occupied molecular orbital (HOMO) and the lowest unoccupied molecular orbital (LUMO) of the molecule and render it fairly soluble in organic solvents.

**Received:** November 26, 2013
**Published:** February 25, 2014




dx.doi.org/10.1021/ja411830x | J. Am. Chem. Soc. 2014, 136, 4593–4598

Herein, we report on the preparation of a covalent few-layer graphene/electron-accepting Pc nanoconjugate *via* copper catalyzed azide−alkyne cycloaddition (CuAAC) "click" chemistry reaction between ethynylphenyl-functionalized graphene and an appropriate Pc bearing one azide and six electron-withdrawing alkylsulfonyl groups. Notably, few-layered graphene was obtained by solvent-assisted exfoliation of graphite following a modification of a procedure recently reported by Tour and co-workers, which relies on the use of chlorosulfonic acid.[14] In addition, a full-fledged and comprehensive assay regarding the electronic features of the resulting nanoconjugate is described.

## RESULTS AND DISCUSSION

In our previous work on covalent few-layer graphene/electron-donating Pc conjugates, we followed the well-known Coleman's procedure, namely sonication of graphite in *N*-methylpyrrolidone (NMP) to obtain dispersions of few-layered graphene.[15] In search for a higher degree of exfoliation, we have now followed a method reported by Tour,[14] which relies on the use of chlorosulfonic acid as the exfoliating agent. This method affords relatively large flakes with no significant defects and a high degree of exfoliation, as demonstrated in the following paragraphs. Therefore, exfoliated graphite (**EG**) was obtained by treating graphite flakes with chlorosulfonic acid for 3 days, followed by centrifugation and quenching of the supernatant with water (see Supporting Information for experimental details).

Transmission electron microscopy (TEM) and atomic force microscopy (AFM) techniques were utilized to shed light onto the nature of **EG**. In the previous work, drop casting of the **EG** suspension and evaporation of the solvent evoked reagglomeration of the flakes. Nevertheless, individual flakes are discernible featuring micrometer-squared sizes (Figure 1). To further corroborate the aforementioned, we performed AFM measurements, which provided additional support for the presence of highly exfoliated graphite. Likewise, AFM reveals flakes with heights as low as 2−3 nm (Figure 1), suggesting the presence of few-layer graphene.

Further insights into the nature of **EG** came from Raman spectroscopy performed with laser excitation at 532 nm.[16] Figure 2 shows a typical Raman spectrum of **EG** together with a statistical distribution of $I(2D)/I(G)$ intensity ratio of 725 measured spectra. Typically, the D-band is discernible at 1340 $cm^{-1}$, while the G- and 2D-bands are centered around 1580 and 2662 $cm^{-1}$, respectively. A statistical distribution of $I(2D)/I(G)$

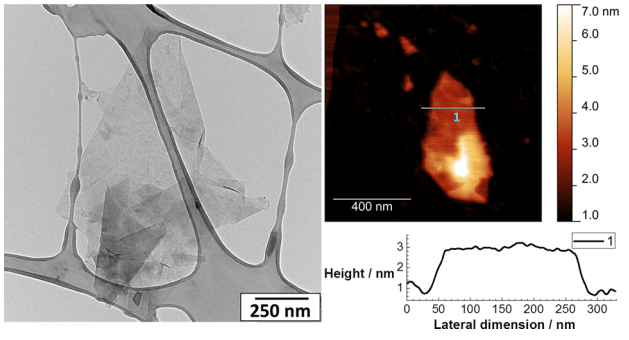


**Figure 1.** TEM image of **EG** on a lacey carbon grid (left) and tapping mode AFM image of **EG** on a $SiO_2$ surface and height profile at position 1 (right).

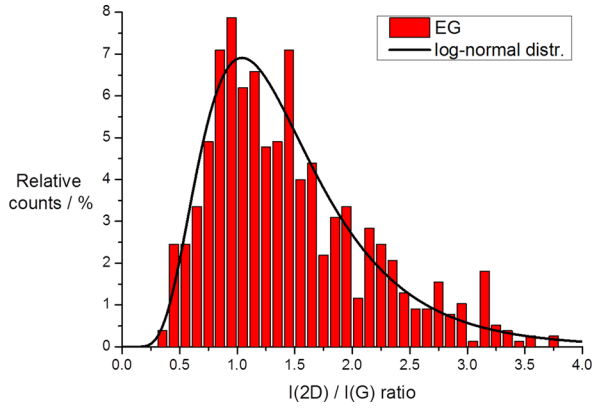


**Figure 2.** (Top) Raman spectrum of **EG**. (Bottom) Histogram with relative counts versus $I(2D)/I(G)$ ratio and the corresponding log-normal distribution. The sample was drop casted from a DMF dispersion onto a $SiO_2$ wafer and was excited at 532 nm.

is best fit by a log-normal distribution function, which peaks at a ratio of 1.1.

For bulk graphite or few-layer-to-multilayer graphene the intensity ratio is expected to be 0.7 or less (Figure S1 in the Supporting Information). In the current case, with such a distribution (Figure 2), 14% of the collected spectra would reveal bulk graphite/few-layer-to-multilayer graphene character, while 86% of the collected spectra would correspond to turbostratic exfoliated graphite/bilayer-to-monolayer graphene,[17] but a major presence of turbostratic exfoliated graphite is more likely. Therefore, in confirmation with TEM and AFM measurements, we conclude that we are dealing mainly with a mixture of turbostratic exfoliated graphite as well as few-layer-to-multilayer graphene. The presence of true monolayers is, however, statistically inferior with maximum $I(2D)/I(G)$ intensity ratios of around 3.0.

Following the confirmation of the successful exfoliation of graphite, we proceeded to its covalent functionalization. First, Pc **1** bearing six 2-ethylhexylsulfonyl chains was synthesized in five steps (Scheme 1). Starting from 4,5-dichlorophthalonitrile, phthalonitrile **3** was prepared by a reaction with 2-ethylhexanethiol, followed by oxidation of the thioether to sulfone using MCPBA. Statistical condensation of phthalonitriles **3** and **4**[18] afforded Pc **5** in 15% yield. Finally, transformation of the alcohol moiety first to bromide (Pc **6**, 70% yield) and then to azide (75% yield) afforded compound **1**.

The procedure for the covalent functionalization of **EG** involved two steps (Scheme 2). To add the required phenylethynyl groups protected as trimethylsilyl ethers (i.e., compound **7**), we converted 4-[(trimethylsilyl)ethynyl]aniline into the corresponding aryl diazonium salt, which reacted *in situ* with a dispersion of **EG** in NMP by means of a microwave-assisted methodology, recently reported by us.[19] After deprotection of **7**, the ethynylphenyl-functionalized conjugate was subjected to CuAAC conditions in NMP with azide-terminated Pc **1** to afford **8**. Nanoconjugates **7** and **8** were characterized by a number of analytical techniques, such as thermogravimetric analysis (TGA), AFM, TEM, Raman spectroscopy, and steady-state and time-resolved spectroscopic techniques.

First, TGA experiments (Figure 3) were performed, which indicated that the initial functionalization with phenylacetylenes in **7** leads to a 7% weight loss at 700 °C, upon excluding weight losses due to adsorbants up to 350 °C. Overall, approximately


dx.doi.org/10.1021/ja411830x | *J. Am. Chem. Soc.* 2014, 136, 4593−4598

**Scheme 1**[a]

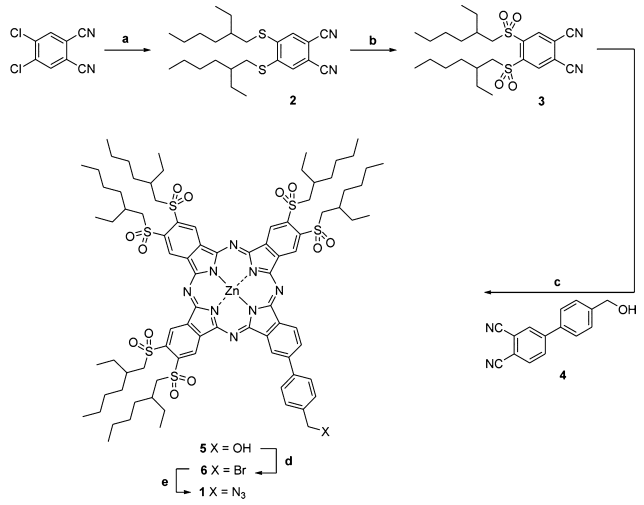


[a]Conditions: (a) 2-ethylhexanethiol, $K_2CO_3$, DMA, 90 °C, 8 h; (b) MCPBA, $CH_2Cl_2$, rt, 18 h; (c) **4**, *o*-DCB/DMF, $Zn(OAc)_2$, 135 °C, 18 h; (d) $CBr_4$, $PPh_3$, $CH_2Cl_2$, room temp, 24 h; (e) $NaN_3$, THF/$H_2O$, 70 °C, 4 h.

**Scheme 2**[a]

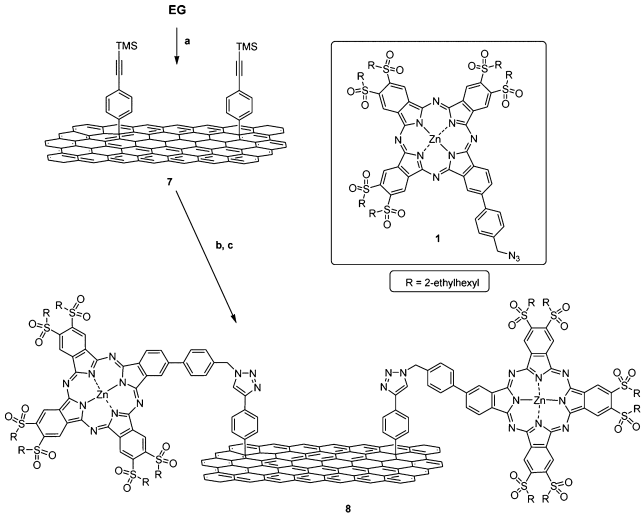


[a]Conditions: (a) 4-[(trimethylsilyl)ethynyl]aniline, isoamyl nitrite, NMP, MW, 80 °C, 1.5 h; (b) TBAF, NMP, 0 °C to room temp, 2 h; (c) Pc **1**, $CuSO_4$, sodium ascorbate, 70 °C, 48 h.

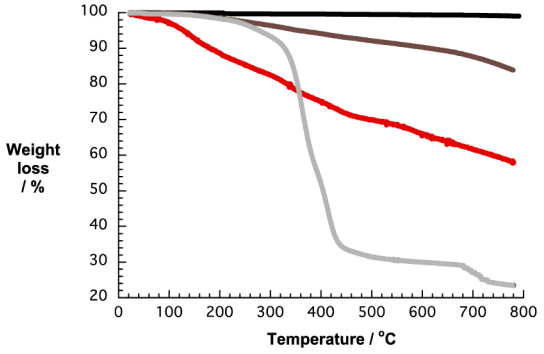


**Figure 3.** TGA curves of graphite (black spectrum), nanoconjugate **7** (brown spectrum), nanoconjugate **8** (red spectrum), and Pc **1** (gray spectrum).

one functional group is present per 200 carbon atoms. The thermogram of **8** shows an additional 13% weight loss, when taking into consideration that Pc **1** gives rise to an overall decomposition of 73% at 700 °C. The observed weight loss corresponds to a functionalization of approximately one Pc every 900 carbon atoms of the exfoliated material. Considering, however, the presence of few-layer graphene, the real Pc-to-carbon ratio at the surface must be assumed to be higher owing to the fact that the inner layers remain unfunctionalized. But, it is very difficult to give an accurate value in light of the heterogeneity of **8**. Remarkably, the degree of functionalization achieved is higher than that reported on the covalent linkage of electron donating Pcs to NMP-assisted **EG**.[6a] We attribute this fact to the use of efficient CuAAC "click" chemistry method to attach the Pcs to the functionalized graphene surface.

In control experiments, **7** was stirred in NMP in the presence of Pc **1** for 48 h. Under these conditions, covalent attachment is unfeasible and the presence of Pc molecules in the graphitic material could only be explained by noncovalent interactions between **1** and the graphene surface. Importantly, TGA experiments with the resulting graphitic material revealed no significant weight loss in the 400 to 700 °C regime. Additional proof for the absence of Pcs on the surface of graphene came from UV−vis spectroscopy. Here, no appreciable Pc absorption was seen. These findings support our initial assumption that the weight loss in **8** is exclusively due to covalently linked Pcs.

Further characterization of **8** was based on AFM and TEM (Figure 4). The graphene flakes were about 1−3 nm in height owing to the presence of folded and intertwined sheets. Along the same lines, TEM reveals folded as well as regularly stacked sheets. The lateral sizes, as confirmed in AFM measurements, are up to 1 $\mu$m. As a matter of fact, the reaggregation of the graphene flakes prior to functionalization (vide supra) was only partially prevented by introducing Pcs, while size and shape of the corresponding flakes are marginally impacted.

Next, **8** was probed by means of Raman spectroscopy upon 532 nm laser excitation. In Figure 5, a representative Raman spectrum and a statistical distribution of $I(2D)/I(G)$ intensity ratio of 2274 measured spectra are displayed. The D-, G-, and 2D-bands of **8** drop casted onto a silicon wafer are centered at around 1345, 1580, and 2687 $cm^{-1}$, respectively. The best fit of the statistical distribution of $I(2D)/I(G)$ by a log-normal distribution function affords a maximum at 0.84. Interestingly, the maximum of the log-normal function shifts to lower values, compared to **EG**. This observation could be rationalized on the basis of increasing defects owing to the covalent functionaliza-

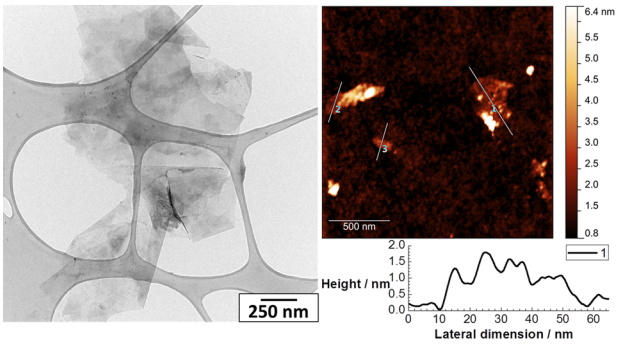


**Figure 4.** TEM image of **8** on a lacey carbon grid (left) and tapping mode AFM image of **8** on a $SiO_2$ surface and height profile at position 1 (right).


dx.doi.org/10.1021/ja411830x | J. Am. Chem. Soc. 2014, 136, 4593−4598

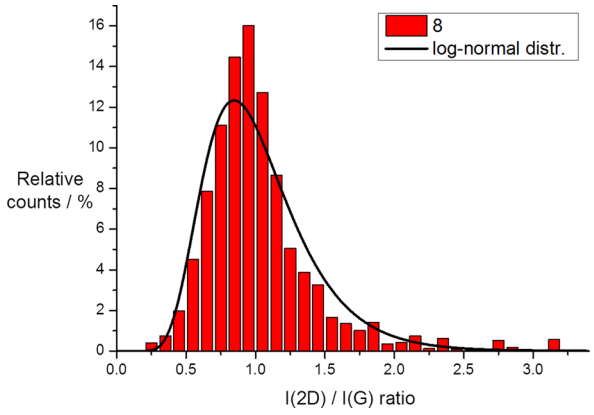


**Figure 5.** (Top) Raman spectrum of **8**. (Bottom) Histogram with relative counts versus $I(2D)/I(G)$ ratio and the corresponding log-normal distribution. The sample was drop casted from a DMF dispersion onto a $SiO_2$ wafer and excited at 532 nm.

tion of **EG**, which has a more profound decrease in intensity of the 2D band[20] in thinner than in thicker flakes.

The ground state features of Pcs in **8** were probed by steady-state absorption experiments with freshly prepared dispersions in DMF *via* ultrasonication. In **1**, the typical Pc Q-band signatures appear in the form of two maxima at 677 and 712 nm, as a consequence of the unsymmetrical functionalization (Figure 6). In the case of **8**, the Soret-band transitions in the range between 300 and 500 nm are superimposed by features that correspond to graphene absorptions and light scattering, but appreciable features that may relate to the distinct and well-resolved Pc Q-bands at 677 and 712 nm are discernible in the spectrum (Figure 6). In stark contrast to previously published Pc–graphene hybrids,[6a] Pc transitions are not bathochromically shifted when compared to the reference, namely Pc **1**. This finding can be rationalized on the basis of weak electronic communication between the basal plane of graphene and Pc due to the rigid nature of the linker. The solution behavior of **8** rather than light scattering, *etc.* was confirmed by performing a series of dilution experiments. In this context, perfect linear relationships between the uniform dilution steps and the resulting decrease in optical density are in perfect agreement with the Lambert–Beer law. The absorption spectrum of **7**, on the other hand, is featureless and is best described as a monotonically decreasing absorption.

Before characterizing the electronic interactions between graphene and Pc molecules in nanoconjugate **8** in terms of energy and/or electron transfer, it was important to determine the spectral features of a Pc reference upon reduction or oxidation. To avoid redox processes associated with the azide group in the Pc precursor **1**, we studied the electrochemical behavior of Pc **5** by cyclic voltammetry experiments in toluene/acetonitrile (4:1 v/v) with 0.1 M tetrabutylammonium hexafluorophosphate ($TBAPF_6$) as electrolyte. In addition, a silver wire, which was calibrated versus the $Fc/Fc^+$ reference redox couple, was used as quasi-reference electrode. The first reversible reduction was detected at −1.1 V, whereas a quasi-reversible oxidation was noted at +0.6 V.

Compared to a $(^tBu)_4ZnPc$ reference (i.e., a typical electron-donating counterpart), which reveals its oxidation at +0.1 V and its reduction at −1.4 V, **5** renders easier to be reduced and more difficult to be oxidized. These differences originate, indeed, from the electron-withdrawing character of the sulfonyl groups. HOMO (−5 eV) and LUMO (−3.3 eV) levels of Pc **5** (and hence, of related hexasulfonylPc derivatives) are consistent with a plausible electron transfer, upon photo-excitation of the Pc component in nanoconjugate **8**, from the Fermi level of graphene/exfoliated graphite (−4.5 eV to −5 eV) to the semioccupied HOMO level of the choromophore (Figure S2 in the Supporting Information). This finding supports our initial assumption that sulfonyl-susbstituted Pcs can be electron-accepting components in ensembles with graphene.

Turning to spectroelectrochemical measurements, a potential of −1.4 V versus Ag-wire was applied for 2 h to reduce **5** and determine the spectral characteristics of its reduced form (Figure 7). New maxima evolve in the region between 400 and 600 nm as well as at 755 nm. These are assigned to the fingerprints of the one electron reduced form of **5**. Additionally, the spectral features are reversibly transformed to those of the nonreduced form upon applying a potential of +0.1 V versus Ag-wire.

In complementary fluorescence assays, emphasis was placed on the fluorescent nature of Pc **1**, which shows a fluorescence maximum at 714 nm, a fluorescence quantum yield of 0.22 ± 0.1 (toluene/pyridine (100:1 v/v)), and a fluorescence lifetime of 2.1 ns (Figure S3 in the Supporting Information). As a consequence of covalently linking **1** to the basal plane of graphene, only weak Pc fluorescence, quenched by more than 90%, was noted for **8** in both steady-state and time-resolved experiments.

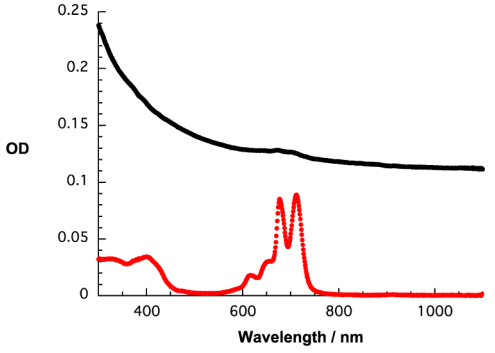


**Figure 6.** Absorption spectra of **1** (red spectrum) and **8** (black spectrum) in DMF.

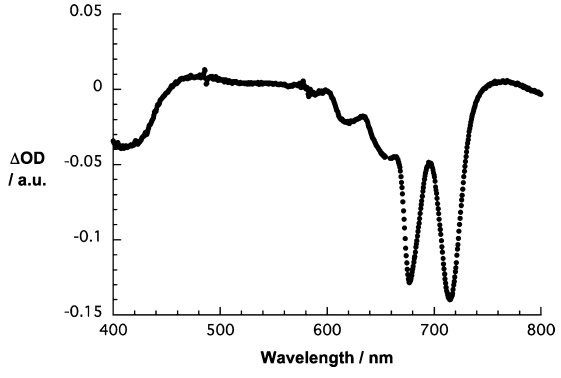


**Figure 7.** Differential absorption spectrum (visible) obtained upon electrochemical reduction of **5** in toluene/acetonitrile (4:1 v/v) with 0.1 M $TBAPF_6$ with an applied potential of −1.4 V versus Ag-wire.


dx.doi.org/10.1021/ja411830x | J. Am. Chem. Soc. 2014, 136, 4593–4598

To gain insights into the product of fluorescence quenching, we employed femtosecond transient absorption measurements following excitation at 387 nm with dispersions of **EG** and **8** in DMF. In reference experiments with **1**, the instantaneous formation of the Pc singlet excited state is discernible throughout the visible and near-infrared section of the solar spectrum (Figure S4 in the Supporting Information). Spectral attributes of the Pc singlet excited transient are minima around 675 and 710 nm, which are good reflections of the ground state bleaching, and maxima at 515 and 850 nm. Owing to their metastability, these features decay rather slowly *via* intersystem crossing (i.e., 1.7 ± 0.2 ns) to the energetically lower lying triplet excited state, showing its signatures for the triplet−triplet absorption at 460 and 790 nm. In the absence of molecular oxygen, the lifetime of the Pc triplet excited state is *ca.* 100 μs. In complementary reference experiments with **EG** in DMF we note, upon excitation at 387 nm, the instantaneous bleach (i.e., 0.5 ± 0.5 ps) of graphene centered transitions in the range of 800 to 1400 nm (Figure S5 in the Supporting Information). For the major decay component of this bleaching, we determined a lifetime of 1.5 ± 0.5 ps corresponding to the reinstating of the graphene ground state.

Finally, turning to **8**, the rapid formation and deactivation of the singlet excited state characteristics of the Pc is discernible within a time window of 1.5 ps (Figure 8). In particular, the spectral range for the Pc centered bleaching extends from 600 to 750 nm, with distinct features at 685 nm that resemble the ground state. Simultaneously with the Pc singlet excited state decay, the formation of a new transient species evolves. The latter maximizes at 570, 636, and 765 nm as well as minimizes at 450 and 680 nm in good agreement with the spectroelectrochemical findings recorded upon one-electron reduction of the Pc. The range beyond 900 nm (i.e., 900−1500 nm) is equally important, which, immediately after the photoexcitation, is dominated by a broad bleaching. Here, new features were noted during the transient decay with a broad maximum ranging from 950 to 1300 nm (Figure 8). Implicit are new valence band holes in graphene. A multiwavelength analysis affords a short-lived and a long-lived component with lifetimes of 1.0 ± 0.5 and 650 ± 100 ps, respectively, in DMF. In line with the aforementioned features we rationalize the kinetics in terms of charge separation and charge recombination.

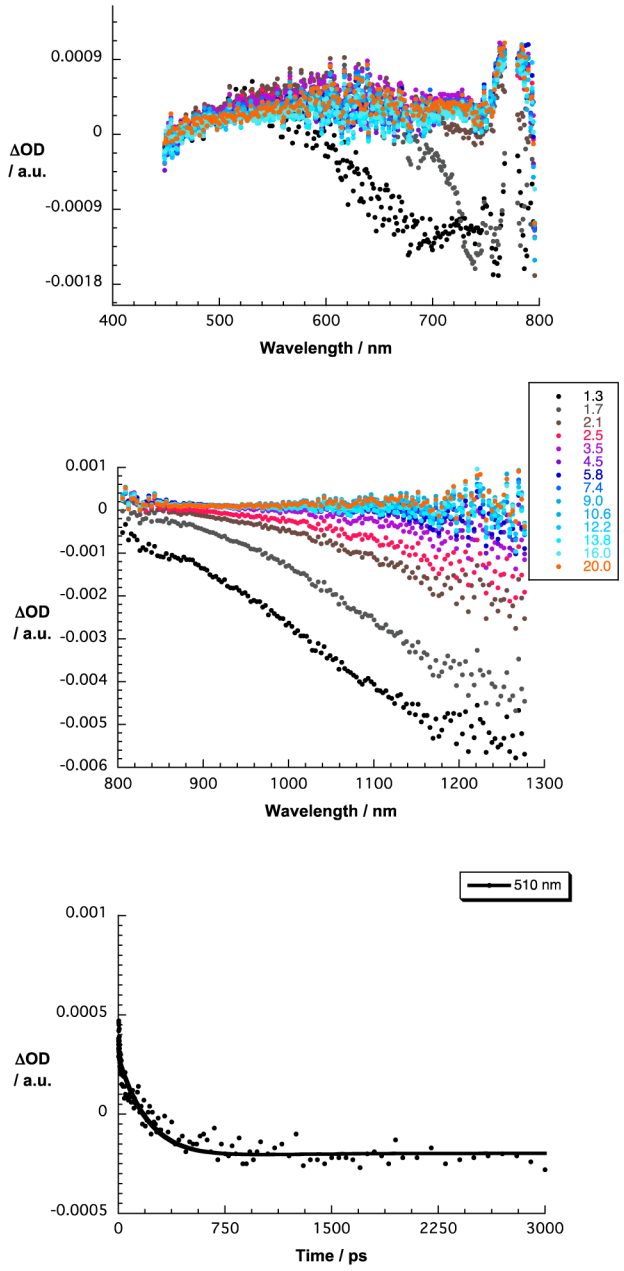


**Figure 8.** (Top) Differential absorption spectra (visible) obtained upon femtosecond pump probe experiments (387 nm) of **8** in DMF with time delays between 1.3 and 20 ps at room temperature (for time delays see Figure legend of middle part). (Middle) differential absorption spectra (visible) obtained upon femtosecond pump probe experiments (387 nm) of **8** in DMF with time delays between 1.3 and 20 ps at room temperature (for time delays see Figure legend). (Bottom) Time absorption profile of the spectra shown in the upper part at 510 nm, monitoring the charge transfer.

## CONCLUSIONS

We present here the first example of an electron-accepting Pc covalently linked to the basal plane of **EG**. Full-fledged microscopic and spectroscopic assays confirm, on one hand, the structure of the resulting electron donor−acceptor conjugate and, on the other hand, the electron transfer evolving from **EG** to the photoexcited Pc component. In terms of electron transfer mechanism, charge separation with 1.0 ± 0.5 ps leads us to assume that a through-space pathway rather than a through bond pathway is operative before charge delocalization within few-layer graphene takes over. Implicit in such a mechanism is a close proximity of the Pcs relative to the basal plane of graphene.

Covalent functionalization introduces $sp^3$ centers within the basal plane of EG, which are expected to impact the charge delocalization and electron donating behavior. Currently, we are directing out efforts to the preparation of noncovalent hybrids using specifically tailored electron-accepting Pcs to study donor−acceptor interactions with nonmodified exfoliated graphene.

## ASSOCIATED CONTENT

### Supporting Information

Experimental section, synthetic procedures, characterization data, and some selected supplementary figures. This material is available free of charge via the Internet at http://pubs.acs.org.


dx.doi.org/10.1021/ja411830x | *J. Am. Chem. Soc.* 2014, 136, 4593−4598

## AUTHOR INFORMATION


### Corresponding Author

tomas.torres@uam.es


### Notes

The authors declare no competing financial interest.

## ACKNOWLEDGMENTS

Financial support from the MICINN and MEC, Spain (CTQ-2011-24187/BQU, PIB2010US-00652, CONSOLIDER-INGENIO 2010 CDS 2007-00010 Nanociencia Molecular, PLE2009-0070), CAM (MADRISOLAR-2, S2009/PPQ/1533), and the Deutsche Forschungsgemeinschaft, the Graduate School of Molecular Science (GSMS), and the Cluster of Excellence: Engineering of Advanced Materials (EAM) is acknowledged. We would like to dedicate this paper to Prof. Fritz Wasgestian on the occasion of his 80th birthday.

## REFERENCES


(1) (a) Hirsch, A.; Englert, J. M.; Hauke, F. *Acc. Chem. Res.* **2013**, *46*, 87. (b) Georgakilas, V.; Otyepka, M.; Bourlinos, A. B.; Chandra, V.; Kim, N.; Kemp, K. C.; Hobza, P.; Zboril, R.; Kim, K. S. *Chem. Rev.* **2012**, *112*, 6156. (c) Sun, Z.; James, D. K.; Tour, J. M. *J. Phys. Chem. Lett.* **2011**, *2*, 2425. (d) Allen, M. J.; Tung, V. C.; Kaner, R. B. *Chem. Rev.* **2010**, *110*, 132.

(2) (a) Englert, J. M.; Dotzer, C.; Yang, G.; Schmid, M.; Papp, C.; Gottfried, J. M.; Steinruck, H.-P.; Spiecker, E.; Hauke, F.; Hirsch, A. *Nat. Chem.* **2011**, *3*, 279. (b) Quintana, M.; Montellano, A.; del Rio Castillo, A. E.; Van Tendeloo, G.; Bittencourt, C.; Prato, M. *Chem. Commun.* **2011**, *47*, 9330. (c) Quintana, M.; Spyrou, K.; Grzelczak, M.; Browne, W. R.; Rudolf, P.; Prato, M. *ACS Nano* **2010**, *4*, 3527.

(3) (a) Castelain, M.; Salavagione, H. J.; Gomez, R.; Segura, J. L. *Chem. Commun.* **2011**, *47*, 7677. (b) Qi, X.; Pu, K. Y.; Li, H.; Zhou, X.; Wu, S.; Fan, Q.-L.; Liu, B.; Boey, F.; Huang, Q.; Zhang, H. *Angew. Chem., Int. Ed.* **2010**, *49*, 9426. (c) Barja, C.; Garnica, M.; Hinarejos, J. J.; Vazquez de Parga, A. L.; Martin, N.; Miranda, R. *Chem. Commun.* **2010**, *46*, 8198.

(4) *The Porphyrin Handbook*; Kadish, K. M., Smith, K. M., Guilard, R., Eds.; Academic Press: San Diego, CA, 2003; Vols. *15*−*20*.

(5) (a) Umeyama, T.; Mihara, T.; Tezuka, N.; Matano, Y.; Stranius, K.; Chukharev, N. V.; Tkachenko, N. V.; Lemetyinen, H.; Noda, K.; Matsushige, K.; Shishido, T.; Liu, Z.; Hirose-Takai, K.; Suenega, K.; Imahori, H. *Chem.*−*Eur. J.* **2012**, *18*, 4250. (b) Karousis, N.; Sandanayaka, A. S. D.; Hasobe, T.; Economopoulos, S. P.; Sarantopoulou, E.; Tagmatarchis, N. *J. Mater. Chem.* **2011**, *21*, 109. (c) Zhang, X.; Hou, L.; Cnossen, A.; Coleman, A. C.; Ivashenko, O.; Rudolf, P.; van Wees, B. J.; Browne, W. R.; Feringa, B. L. *Chem.—Eur. J.* **2011**, *17*, 8957. (d) Xu, Y.; Zhao, L.; Bai, H.; Hong, W.; Li, Ch.; Shi, G. *J. Am. Chem. Soc.* **2009**, *131*, 13490. (e) Xue, T.; Jiang, S.; Qu, Y.; Su, Q.; Cheng, R.; Dubin, S.; Chiu, C.-Y.; Kaner, R.; Huang, Y.; Duan, X. *Angew. Chem., Int. Ed.* **2012**, *51*, 3822. (f) Kiessling, D.; Costa, R. D.; Katsukis, G.; Malig, J.; Lodermeyer, F.; Feihl, S.; Roth, A.; Wibmer, L.; Kehrer, M.; Volland, M.; Wagner, P.; Wallace, G. G.; Officer, D. L.; Guldi, D. M. *Chem. Sci.* **2013**, *4*, 3085. (g) Malig, J.; Stephenson, A. W.; Wagner, P.; Wallace, G. G.; Officer, D. L.; Guldi, D. M. *Chem. Commun.* **2012**, *48*, 8745.

(6) (a) Ragoussi, M. E.; Malig, J.; Katsukis, G.; Butz, B.; Spiecker, E.; de la Torre, G.; Torres, T.; Guldi, D. M. *Angew. Chem., Int. Ed.* **2012**, *51*, 6421. (b) Malig, J.; Jux, N.; Kiessling, D.; Cid, J.-J.; Vazquez, P.; Torres, T.; Guldi, D. M. *Angew. Chem., Int. Ed.* **2011**, *50*, 3561. (c) Karousis, N.; Ortiz, J.; Ohkubo, K.; Hasobe, T.; Fukuzumi, S.; Sastre-Santos, A.; Tagmatarchis, N. *J. Phys. Chem. C* **2012**, *116*, 20564. (d) Dirian, K.; Herranz, M. A.; Katsukis, G.; Malig, J.; Rodriguez-Perez, L.; Romero-Nieto, C.; Strauss, V.; Martin, N.; Guldi, D. M. *Chem. Sci.* **2013**, *4*, 4335.

(7) (a) Bottari, G.; Suanzes, J. A.; Trukhina, O.; Torres, T. *J. Phys. Chem. Lett.* **2011**, *2*, 905. (b) Umeyama, T.; Imahori, H. *J. Phys. Chem. C* **2013**, *117*, 3195. (c) Malig, J.; Jux, N.; Guldi, D. M. *Acc. Chem. Res.* **2013**, *46*, 53.

(8) (a) Oelsner, C.; Schmidt, C.; Hauke, F.; Prato, M.; Hirsch, A.; Guldi, D. M. *J. Am. Chem. Soc.* **2011**, *133*, 4580. (b) D'Souza, F.; Sandanayaka, A. S. D.; Ito, O. *J. Phys. Chem. Lett.* **2010**, *1*, 2586. (c) Ohtani, M.; Fukuzumi, S. *Chem. Commun.* **2009**, 4997. (d) Boul, P. J.; Cho, D.-G.; Aminur Rahman, G. M.; Marquez, M.; Ou, Z.; Kadish, K. M.; Guldi, D. M.; Sessler, J. L. *J. Am. Chem. Soc.* **2007**, *129*, 5683. (e) Ince, M.; Bartelmess, J.; Kiessling, D.; Dirian, K.; Martínez-Díaz, M. V.; Torres, T.; Guldi, D. M. *Chem. Sci.* **2012**, *3*, 1472.

(9) (a) Kozhemyakina, N. V.; Englert, J. M.; Yang, G.; Spiecker, E.; Schmidt, C. D.; Hauke, F.; Hirsch, A. *Adv. Mater.* **2010**, *22*, 5483. (b) Pinto, H.; Jones, R.; Goss, J.; Briddon, P. *J. Phys.: Condens. Matter* **2009**, *21*, 402001. (c) Chen, W.; Chen, S.; Qi, D. C.; Gao, X. Y.; Wee, A. T. S. *J. Am. Chem. Soc.* **2007**, *129*, 10418. (d) Voggu, R.; Das, B.; Rout, C. S.; Rao, C. *J. Phys.: Condens. Matter* **2008**, *20*, 472204. (e) Varghese, N.; Ghosh, A.; Voggu, R.; Ghosh, S.; Rao, C. *J. Phys. Chem. C* **2009**, *113*, 16855. (f) Hao, R.; Qian, W.; Zhang, L.; Hou, Y. *Chem. Commun.* **2008**, 6576.

(10) Costa, R. D.; Malig, J.; Brenner, W.; Jux, N.; Guldi, D. M. *Adv. Mater.* **2013**, *25*, 2600.

(11) Bottari, G.; de la Torre, G.; Guldi, D. M.; Torres, T. *Chem. Rev.* **2010**, *110*, 6768.

(12) (a) Yang, K.; Xiao, W. D.; Jiang, Y. H.; Zhang, H. G.; Liu, L. W.; Mao, J. H.; Zhou, H. T.; Du, S. X.; Gao, H.-J. *J. Phys. Chem. C* **2012**, *116*, 14052. (b) Hämäläinen, S. K.; Stepanova, M.; Drost, R.; Liljeroth, P.; Lahtinen, J.; Sainio, J. *J. Phys. Chem. C* **2012**, *116*, 20433. (c) Scardamaglia, M.; Lisi, S.; Lizzit, S.; Baraldi, A.; Larciprete, R.; Mariani, C.; Betti, M. G. *J. Phys. Chem. C* **2013**, *117*, 3019.

(13) Zhang, Y.; Ma, P.; Zhu, P.; Zhang, X.; Gao, Y.; Qi, D.; Bian, Y.; Kobayashi, N.; Jiang, J. *J. Mater. Chem.* **2011**, *21*, 6515.

(14) Behabtu, N.; Lomeda, J. R.; Green, M. J.; Higginbotham, A. L.; Sinitskii, A.; Kosynkin, D. V.; Tsentalovich, D.; Nicholas, A.; Parra-Vasquez, G.; Schmidt, J.; Kesselman, E.; Cohen, Y.; Talmon, Y.; Tour, J. M.; Pasquali, M. *Nat. Nanotechnol.* **2010**, 406.

(15) Hernandez, Y.; Nicolosi, V.; Lotya, M.; Blighe, F. M.; Sun, Z.; De, S.; McGovern, I. T.; Holland, B.; Byrne, M.; Gun'Ko, Y. K.; Boland, J. J.; Niraj, P.; Duesberg, G.; Krishnamurthy, S.; Goodhue, R.; Hutchison, J.; Scardaci, V.; Ferrari, A. C.; Coleman, J. N. *Nat. Nanotechnol.* **2008**, *3*, 63.

(16) Englert, J. M.; Vecera, P.; Knirsch, K. C.; Schäfer, R. A.; Hauke, F.; Hirsch, A. *ACS Nano* **2013**, *7*, 5472.

(17) (a) Ferrari, A. C.; Meyer, J. C.; Scardaci, V.; Casiraghi, C.; Lazzeri, M.; Mauri, F.; Piscanec, S.; Jiang, D.; Novoselov, K. S.; Roth, S.; Geim, A. K. *Phys. Rev. Lett.* **2006**, *97*, 187401. (b) Green, A. A.; Hersam, M. C. *J. Phys. Chem. Lett.* **2009**, *1*, 544.

(18) Ballesteros, B.; Campidelli, S.; de la Torre, G.; Ehli, C.; Guldi, D. M.; Prato, M.; Torres, T. *Chem. Commun.* **2007**, 2950.

(19) Ragoussi, M.-E.; Casado, S.; Ribeiro-Viana, R.; de la Torre, G.; Rojo, J.; Torres, T. *Chem. Sci.* **2013**, 4035.

(20) (a) Niyogi, S.; Bekyarova, E.; Hong, J.; Khizroev, S.; Berger, C.; de Heer, W.; Haddon, R. C. *J. Phys. Chem. Lett.* **2011**, *2*, 2487. (b) Cancado, L. G.; Jorio, A.; Martins Ferreira, E. H.; Stavale, F.; Achete, C. A.; Capaz, R. B.; Moutinho, M. V. O.; Lombardo, A.; Kulmala, T. S.; Ferrari, A. C. *Nano Lett.* **2011**, *11*, 3190.